Competition for electrons favors N_2O reduction in denitrifying *Bradyrhizobium* isolates

Gao Y[1*], Mania D[1], Mousavi SA[2], Lycus P[1], Arntzen M[1], Woliy K[1†], Lindström K[2], Shapleigh JP[3], Bakken LR[1] and Frostegård Å[1*]

[1] Faculty of Chemistry, Biotechnology and Food Sciences, Norwegian University of Life Sciences, Aas, Norway

[2] Ecosystems and Environment Research programme, Faculty of Biological and Environmental Sciences, and Helsinki Institute of Sustainability Science (HELSUS), University of Helsinki, Finland

[3] Department of Microbiology, Cornell University, Ithaca, New York, USA

[†]Present address: Department of Biology, Hawassa University, Hawassa, Ethiopia

[*]Corresponding author, E-mail asa.frostegard@nmbu.no; Tel. (+47) 67232473.

Summary

Bradyrhizobia are common members of soil microbiomes and known as N_2-fixing symbionts of economically important legumes. Many are also denitrifiers, which can act as sinks or sources for N_2O. Inoculation with compatible rhizobia is often needed for optimal N_2-fixation, but the choice of inoculant may also have consequences for N_2O emission. Here, we analyzed the phylogeny

and denitrification capacity of *Bradyrhizobium* strains, most of them isolated from peanut-nodules. All were dinitrifiers, but only ~1/3 could reduce N_2O while most others were net N_2O producers. The N_2O-reducing isolates showed strong preference for N_2O- over NO_3^--reduction. Such preference was also observed in a study of other bradyrhizobia and tentatively ascribed to competition between the electron pathways to Nap (periplasmic NO_3^- reductase) and Nos (N_2O reductase). Another possible explanation is lower abundance of Nap than Nos. Here, proteomics revealed that Nap was instead more abundant than Nos, supporting the hypothesis that the electron pathway to Nos outcompetes that to Nap. In contrast, *Paracoccus denitrificans,* which has membrane-bond NO_3^- reductase (Nar), reduced N_2O and NO_3^- simultaneously. We propose that the control at the metabolic level, favoring N_2O reduction over NO_3^- reduction, applies also to other denitrifiers carrying Nos and Nap but lacking Nar.

Originality-Significance Statement

This study extends the current knowledge on denitrification in bradyrhizobia, which mostly originates from studies of one model strain, by investigating the denitrification phenotypes of a diverse collection of Bradyrhizobium isolates. Only 1/3 of them could reduce N_2O while the others were net sources for this potent greenhouse gas. All N_2O-reducers showed strong preference for N_2O over NO_3^-. We revealed by proteomics that this was not explained by differences in the abundances of Nap (periplasmic nitrate reductase) and Nos (N_2O reductase), which strengthens our hypothesis (Mania *et al*., 2020) of a metabolic control mechanism by which Nos competes efficiently with Nap for electrons, making these organisms strong sinks for N_2O. The findings highlight the potential importance of these organisms as N_2O sinks in natural

45 and agricultural ecosystems and pinpoint the need to take N_2O reduction into account, along
46 with N_2-fixation effectiveness, when searching for strains suitable for production of inoculants.
47

48 **Introduction**

49 Emissions of nitrous oxide (N_2O), the third most important anthropogenic greenhouse gas, have
50 been rising steadily during the past 150 years. Predictions for the rest of the century show either
51 continued N_2O emission increases or rates of decrease slower than the decreases occurring in
52 CO_2 emissions (Rogelj *et al*., 2018; Thompson *et al.*, 2019). Agriculture is the main source of
53 anthropogenic N_2O emissions, with denitrification playing the major role in most soils (Thomson
54 *et al.*, 2012). The primary cause of the emissions is excessive use of synthetic fertilizers (Reay *et*
55 *al.*, 2012; Thompson *et al.*, 2019; Tian *et al.*, 2020), but cultivation of legumes also contributes
56 substantially with a global average of 1.29 (range 0.03-7.09) kg N_2O-N ha^{-1} $year^{-1}$ while the
57 corresponding estimate for fertilized agricultural fields was 3.22 (range 0.09-12.67) (Jensen *et al.*,
58 2012). In both cases, the ultimate driver of the emission is input of reactive nitrogen which
59 undergoes a series of redox reactions and eventually returns to the atmosphere as N_2O or N_2.
60 Our aim should be to minimize the N_2O/N_2 emission ratio of the system (Schlesinger, 2009). To
61 achieve this, novel mitigation options beyond "good agronomic practice" will be needed
62 (Davidson and Kanter, 2014). Several technical abatement options have been suggested,
63 including precision fertilization and use of nitrification inhibitors (Winiwarter *et al.*, 2018).
64 An alternative strategy is to enhance the populations of N_2O reducing microorganisms in the
65 soil. Selective *in situ* stimulation of N_2O reducing, indigenous soil organisms appears unrealistic,
66 while some options for the addition of N_2O reducing microbes may be feasible. One is the

67 suggestion to inoculate soybeans with rhizobia that are not only efficient N_2-fixers but also have
68 the capacity to reduce N_2O (Hénault and Revellin, 2011; Itakura *et al.*, 2013; Akiyama *et al.*, 2016).
69 At present, N_2O reduction is not taken into account when screening strains for their suitability as
70 inoculants and, in fact, several of the commercial inoculants currently used are only partial
71 denitrifiers (Zilli *et al.*, 2019). For example, only one of the five *Bradyrhizobium* strains most
72 commonly used as soybean inoculants in South America could reduce N_2O (Obando *et al.*, 2019).
73 The growing global need for plant-based proteins is expected to require new areas to be used for
74 legume cropping and will likely increase the demand for new legume varieties. Not all
75 combinations of legume cultivar and rhizobial strain result in an efficient symbiosis (Thrall *et al.*,
76 2011; Woliy *et al*, 2019). Importantly, indigenous soil populations of rhizobia may not be
77 compatible with a certain legume crop, especially if it has not been grown in that area before.
78 Therefore, the expansion of legume cropping is creating an increasing demand for a wider variety
79 of inoculants to ensure nodulation and optimal N_2 fixation efficacy (Santos *et al.*, 2019). This
80 offers a golden opportunity to mitigate N_2O emissions, providing that the inoculants are selected
81 among rhizobial strains that can reduce N_2O.

82 The purpose of the present study was to determine how denitrification phenotypes vary
83 across taxonomically diverse groups of bradyrhizobia, with particular focus on their capacity for
84 N_2O reduction, and to understand cellular mechanisms that make these organisms potential sinks
85 for N_2O. We determined the phylogenetic position of a set of *Bradyrhizobium* strains, obtained
86 from different culture collections, and analyzed their capacity for denitrification. Most of the
87 strains were isolated from nodules of peanut plants (*Arachis hypogaea*) growing in different
88 regions of China. Peanut is the fourth most important legume crop globally, with China being the

89 main producer (Arya *et al.*, 2016). We also included some bradyrhizobia from other parts of the
90 world, isolated from peanut and other legumes.

91 Several taxonomic groups within the genus *Bradyrhizobium* have been reported to denitrify
92 with many strains having truncated denitrification pathways lacking one or more of the steps
93 (Sameshima-Saito *et al.,* 2004; Zilli *et al*., 2019; Mania *et al*., 2020). A complete denitrification
94 pathway in bradyrhizobia comprises the periplasmic reductase Nap for dissimilatory NO_3^-
95 reduction, encoded as a part of the *napEDABC* operon; the Cu-containing nitrite reductase NirK
96 encoded by *nirK* only or as a part of the *nirKV* operon, although cd_1-type NirS nitrite reductase
97 has also been reported (Sánchez and Minamisawa, 2018); the cytochrome *c* dependent nitric
98 oxide reductase cNor *(norCBQD* operon); and a clade I N_2O reductase Nos (*nosRZDYFLX* operon)
99 (Velasco *et al.*, 2001;Mesa *et al.*, 2002; Delgado *et al.*, 2003; Velasco *et al.*, 2004; Bedmar *et al.*,
100 2005). While the bradyrhizobia, along with several other denitrifiers, only have the periplasmic
101 Nap for dissimilatory NO_3^- reduction, other denitrifiers have the membrane-bound Nar, or both.
102 Nap is a periplasmic heterodimer (NapAB) consisting of the small electron transfer subunit NapB
103 and the catalytic NapA, which draws electrons from quinol via the membrane-bound *c*-type
104 tetrahaeme cytochrome NapC. Nar is a three-subunit enzyme (NarGHI) anchored in the
105 membrane by NarI, which is a transmembrane protein that draws electrons from quinol to the
106 catalytic NarG via NarH, both facing the cytoplasm (Richardson, 2000; Richardson *et al.*, 2001).
107 Nir, Nor and Nos receive electrons from the bc_1 complex via periplasmic small c-type cytochromes
108 (Berks *et al.*, 1995; Zumft, 1997). Clade I type Nos reductase may in addition draw electrons from
109 quinol via the membrane bound NosR (Zhang *et al.*, 2019).

110 In a recent study, Mania *et al.* (2020) screened strains within the genus *Bradyrhizobium* for
111 their denitrification phenotype. Most of them could perform two or more of the denitrification
112 steps, but only half of them could reduce N_2O. All the N_2O reducing strains displayed the same
113 strong preference for N_2O over NO_3^- reduction when incubated under anoxic conditions, which
114 was suggested to be due to competition between the electron pathways to Nap and Nos. The
115 quantification of denitrification gene transcripts showed 5-8 times lower transcript numbers of
116 *nap* compared to *nos,* however. Therefore, it could not be excluded that the phenomenon is due
117 to low abundance of Nap compared to Nos. Here we have investigated the denitrification geno-
118 and phenotypes for another collection of *Bradyrhizobium* isolates and deepened our
119 understanding of the competition for electrons between Nap and Nos by refined analyses of the
120 electron flow kinetics, in combination with the determination of the relative amounts of Nap and
121 Nos by proteomics. In addition, we compared the denitrification kinetics of the bradyrhizobia
122 with the denitrification model bacterium *Paracoccus denitrificans*, which holds a complete
123 denitrification pathway including both Nap and Nar (Zumft, 1997; Richardson, 2000). The results
124 showed that in all bradyrhizobia with complete denitrification, NO_3^- reduction was almost
125 completely hampered in the presence of N_2O. The proteomics analysis provided evidence that
126 this was not due to a low abundance of Nap, also showing that transcript abundance cannot be
127 directly translated into corresponding protein abundance. As expected, the NarG carrying *P.*
128 *denitrificans* showed a different denitrification phenotype with simultaneous reduction of NO_3^-
129 and N_2O.
130
131 **Results**

132 *Phylogenetic distribution of denitrifying bradyrhizobia*

133 The phylogenetic position of the 23 test strains was determined by MLSA analysis of four protein-
134 coding housekeeping genes (*atpD-glnII-recA-rpoB*) (Fig. 1). The analysis comprised 78
135 bradyrhizobial strains and included all hitherto described *Bradyrhizobium* reference species. All
136 but one of the 23 test strains listed in Table 1 were assigned to the *Bradyrhizobium japonicum*
137 supergroup (Fig. 1). The exception was *Bradyrhizobium lablabi* HAMBI 3052^{T}, which is a member
138 of the *Bradyrhizobium jicamae* supergroup according to the new genome-based taxonomy of
139 bradyrhizobia proposed by Avontuur *et al.* (2019). The test strains were placed in 11 lineages
140 (clades A-K) with high posterior probability (PP=1.00). Most test strains were clustered within the
141 clades of seven diverse bradyrhizobial species. Strains *Bradyrhizobium* sp. HAMBI 2134 and 2142
142 formed a monophyletic cluster (clade G) with high posterior probability (1.00). *Bradyrhizobium*
143 sp. strain HAMBI 2116 was accommodated in a lineage (clade A) distant from other bradyrhizobia.
144 The phylogenetic relationships revealed by the four-gene MLSA tree (Fig. 1) showed good
145 correspondence with the results from an analysis of all the HAMBI strains using the GTDB Tool
146 kit (Fig. S1). In both trees strains HAMBI 2299, 2153 and 2116 were most closely related to the
147 reference species *B. yuanmingense*; strains HAMBI 2125 (and 2126) and 2127 were closest to *B.*
148 *ottawaense*; strain HAMBI 2130 was closest to *B. shewense*; strains HAMBI 2115 was closest to
149 *B. japonicum* USDA6; strains HAMBI 2128 (as well as HAMBI 2129 and 2150, Table S1) were
150 closest to *B. arachidis*; strain HAMBI 3052 was closest to *B. lablabi.* Strains HAMBI 2149, 2133,
151 2136, 2137, 2151 and 2152 formed one cluster in the GTDB tree together with *B. japonicum* USDA
152 135. This cluster was close to *B. liaoningense*, as also found in the MLSA analysis (Clade F, Fig. 1),

153 which did not include *B. japonicum* USDA 135. Strains HAMBI 2134 (and 2135, Table S1) and 2142
154 formed a separate cluster in both trees.

155 We originally included 21 isolates from the HAMBI culture collection in our study, all
156 deposited with different strain names. Pairwise whole genome comparisons revealed that some
157 strains were very similar with ANI values >99.2% and in most cases >99.9 % (Table S1), which was
158 also supported by the clustering of similar strains in the GTDB tree (Fig. S1). Since the strains
159 within such clusters with ANI values >99% also showed practically identical denitrification
160 phenotypes, we present the result for only one of the strains in each such cluster in the main
161 paper, and the results for the others as supplementary information.

162 The denitrification end-product analysis showed that all test strains were denitrifiers, able to
163 reduce NO_3^- and/or NO_2^- to NO, N_2O or N_2. Seven of the 19 strains tested for denitrification in the
164 present study were complete denitrifers that reduced NO_3^- to N_2. The four Ethiopian strains
165 AC87j1, AC86d2, AC101b and AC70c were determined earlier to be complete denitrifiers (Mania
166 *et al*. 2020). All complete denitrifiers except *B. lablabi* (clade K) belonged to the *B. japonicum*
167 supergroup and were positioned in clades E, H, I and J. The clades E, H and J represented the
168 species *B. guangxiense*, *B. ottawaense* and *B. shewense*, respectively. Clade I, accommodating
169 strains *Bradyrhizobium* sp. HAMBI 2125 and AC70c, formed a separate, monophyletic group. The
170 other test strains had truncated denitrification pathways and were able to reduce NO_3^- and NO_2^-
171 to NO (5 strains) or N_2O (7 strains). The seven strains having N_2O as end-product were distributed
172 in clades A, C, D and G. Three strains grouped with *B. arachidis* in clade C*. Bradyrhizobium* sp.
173 strain HAMBI 2115 was placed in clade D along with *B. japonicum* USDA6^T. Three strains were
174 accommodated in clades A and G, neither of which included any of the hitherto described

175 *Bradyrhizobium* species. The strains with NO as denitrification end-product were found in clades
176 B, C and F, which also harbored the species *B. yuanmingense*, *B. arachidis* and *B. liaoningense*,
177 respectively. Strains HAMBI 2153 and 2149, as well as the strains highly similar to HAMBI 2149
178 (Table S1), were also examined using detailed gas kinetics to further examine whether they could
179 reduce NO (Fig. S2). Like in the end-product investigation they produced large amounts of NO
180 (14-15 µmol flask^{-1}) while no reduction of NO or N_2O was detected (Fig. S2).
181
182 *Consistency between denitrification gene operons and end products*
183 The genetic potential for denitrification, based on whole genome sequencing, and the
184 corresponding phenotype, determined by end-point analysis and gas kinetics, were compared
185 for 13 strains (Table S2), as well as for isolates with genomes with ANI values >99.2% to these
186 strains (Table S1). The five strains able to reduce NO_3^- to N_2 had complete operons for all four
187 reduction steps. For most of the other strains, with NO or N_2O as denitrification end -products,
188 the lack of a function was explained by complete lack of the corresponding operon. However,
189 two strains (HAMBI 2153 and HAMBI 2299) showed a discrepancy between denitrification
190 genotype and phenotype. They were apparently unable to reduce NO and accumulated µM
191 concentrations of NO, despite having the *nor* operon. Comparison of these strains with strains
192 having functional NO reduction revealed that strain HAMBI 2153 had a frame shift in *norB*, while
193 *norQ* was not in the correct reading frame. Strain HAMBI 2299 carried *nap, nir* and *nor* operons
194 with all expected genes present. The end-point analysis of this strain showed that after 10 days
195 of incubation with 1 mM NO_3^-, 0.5 mM NO_2^- and 1 ml N_2O in headspace, it had produced toxic

196 levels (>10 µM) of NO. Inspection of the amino acid sequences did not reveal any obvious
197 explanations for lack of Nor activity.
198
199 *All N_2O-reducing* Bradyrhizobium *strains preferred N_2O over NO_3^- as electron acceptor*
200 To determine if the complete denitrifiers showed a similar, strong preference for N_2O over NO_3^-
201 as reported by Mania *et al.* (2020) for other *Bradyrhizobium* strains, detailed gas kinetics was
202 analyzed. The results showed remarkably similar kinetics for all strains during and after the
203 transition from aerobic to anaerobic respiration in flasks to which N_2O had been added to the
204 headspace (Figs 2A, S3, S4, S5). Strain HAMBI 2125 was chosen as a representative for the
205 complete denitrifiers. The NO_2^- concentration in cultures of this strain was measured along with
206 the gas kinetics (Figs 2A, S3), allowing the estimation of NO_3^- concentrations by N-mass balance.
207 The first phase, marked in blue, was dominated by O_2 respiration. When the O_2 concentration
208 in the medium reached 4.6 µM, some NO_3^- reduction took place, measured as a slight
209 accumulation of NO_2^- and NO (0.7 and 1.7 µmol; not clearly visible in the figure due to scaling).
210 The small but significant decrease in N_2O during the aerobic phase was caused by sampling losses,
211 not by N_2O reduction or other reactions, as explained in Fig. S6. The same is seen for experiments
212 presented in Figs. 2B and S3-S5. Reduction of exogenous N_2O started when the O_2 concentration
213 in the liquid was approximately 3.0 µM and rapidly reached a rate of 10.4 ± 1.2 µmol N flask^{-1} h^{-}
214 ^{1}, matching the corresponding N_2 production rate of 9.7 ± 1.0 µmol N flask^{-1} h^{-1}. This phase of
215 rapid and stoichiometric reduction of N_2O to N_2, marked in pink, lasted until most of the
216 exogenous N_2O was reduced. No NO_3^--reduction took place during reduction of the exogenous
217 N_2O. When the exogenous N_2O was depleted, the rate of NO_3^- reduction increased and the rate

218 of N_2 production decreased instantaneously to 2.22 ± 0.18 µmol flask^{-1} h^{-1} (phase marked in
219 green). When NO_3^- reduction started, the NO_2^- concentration increased sharply and reached
220 approximately 200-350 µM (9.8-17.4 µmol flask^{-1}), accounting for 20-35% of the initial 50 µmol
221 NO_3^--N. The N_2 curve for strain HAMBI 2125 reached a stable plateau at 123 µmol N_2-N, which
222 accounts for the sum of N_2O- and NO_3-N present initially. The same experiment was conducted
223 with other strains, but without measuring NO_2^- (Figs S4, S5), and they all showed the same fast
224 stoichiometric conversion of N_2O to N_2 and a subsequent slower production of N_2 from NO_3^-,
225 lasting until the N_2O+NO_3^--N was completely recovered as N_2-N. Strain HAMBI 2125 controlled
226 NO during the entire incubation period, reaching a small peak of 11 nmol flask^{-1} (6.9 nM in the
227 liquid) around 41 hpi. For the other strains NO concentrations never exceeded 50 nM, and most
228 strains kept NO concentrations <20 nM during the entire incubation (Figs 2A, S3, S4, S5).
229
230 *Nar carrying* Paracoccus denitrificans *showed no preference for N_2O over NO_3^-*
231 In accordance with our hypothesis, the Nar carrying *P. denitrificans* reduced NO_3^- simultaneously
232 with the exogenously supplied N_2O, indicating no hampering of NO_3^- reduction by N_2O (Fig. 2B).
233 In contrast to all the examined *Bradyrhizobium* strains (Figs 2A, S3, S4, S5), *P. denitrificans* started
234 to reduce NO_3^- and headspace N_2O concomitantly when the O_2 concentration was close to
235 depletion and stoichiometrically accumulated NO_2^- from NO_3^- reduction. Nitrite reduction and
236 emergence of NO started when most of the NO_3^- had been reduced to NO_2^-.
237
238 *Cell specific electron flow rates*

239 The measured gas- and NO_2 kinetics were used to estimate the electron flow rates to the various
240 reductase (µmol e^- $flask^{-1}$ h^{-1}) for each time increment between gas samplings. To convert these
241 rates to cell specific electron flow rates (fmol $cell^{-1}$ h^{-1}), we needed estimates of the cell density
242 throughout an incubation. For this, we used cumulated electron flow to the various electron
243 acceptors (calculated from the gas- and NO_2^-- measurements), and the cell yield per mol electrons
244 to each electron acceptor, which was determined in a separate experiment (see Experimental
245 procedures and Fig. 5). In *Bradyrhizobium* strain HAMBI 2125 (Fig. 2C), the cell specific electron
246 flow was sustained at a more or less constant level (5-6 fmol e^- $cell^{-1}$ h^{-1}) through the transition
247 from respiring O_2 to respiring N_2O, until the external N_2O was depleted (phases marked blue and
248 pink in the corresponding gas kinetics Fig. 2A), but declined to ~3-4 fmol e^- $cell^{-1}$ h^{-1} when
249 depending on the activity of Nap. In *P. denitrificans* (Fig. 2D) there was instead a simultaneous
250 electron delivery to Nar and Nos during the phase when exogenous N_2O was being reduced
251 (marked pink in the corresponding gas kinetics, Fig. 2B). This was later followed by electron flow
252 to Nir, Nor and Nos, after the depletion of nitrate. The cell specific respiratory metabolism was
253 10-13 fmol e^- $cell^{-1}$ h^{-1} during the phase dominated by aerobic respiration, then increased to 15-
254 16 fmol e^- $cell^{-1}$ h^{-1} when respiring NO_3^- and N_2O, followed by a decrease to approximately 8 fmol
255 e^- $cell^{-1}$ h^{-1} during respiration of the accumulated NO_2^-.
256
257 *Injection of N_2O to actively denitrifying cultures resulted in an immediate arrest of NO_3^- reduction*
258 To investigate whether the preferred electron flow to N_2O in the foregoing experiments could be
259 explained by regulation at the transcriptional level (i.e. early expression of *nos*), N_2O was injected
260 into a culture that was actively reducing NO_3^- to N_2. A transcriptional regulation would not result

261 in an immediate switch to the exogenous N_2O as electron acceptor but would instead be seen as
262 a simultaneous reduction of all N-oxides present. This was tested on strain HAMBI 2125 (Fig. 3).
263 The cultures were incubated in flasks containing YMB with 2 mM initial NO_3^-, and with 1% O_2 but
264 without exogenous N_2O in the headspace. Denitrification (from NO_3^- reduction) commenced
265 when O_2 reached 4.3 µM and proceeded at a rate of 2.6 ± 0.4 µmol N flask^{-1} h^{-1}. At 32 hpi, when
266 the cells were actively reducing NO_3^- to N_2, approximately 300 µmol N_2O-N was injected. This led
267 to a complete suppression of NO_3^- reduction and rapid decline in NO accumulation. The measured
268 N_2 production rate was similar to the measured N_2O reduction rate (23.9 ±3.6 and 26.4 ±3.6 µmol
269 N flask^{-1} h^{-1}, respectively). The NO_3^- reduction recovered upon depletion of external N_2O,
270 reflected in an increase in NO and an N_2 production rate similar to that before the N_2O injection.
271 In an additional experiment, including all seven N_2O-reducing strains, exogenous N_2O was
272 present in the headspace from the start of the incubation (Fig. S5). As expected from the first
273 experiment (Fig. 2A), the exogenous N_2O was rapidly reduced, followed by NO_3^- reduction to N_2
274 at a slower rate. A second injection of N_2O into the actively denitrifying cultures resulted in an
275 immediate increase in the N_2 production rate, comparable with that during reduction of the initial
276 N_2O. These results supported the notion that N_2O was preferred as electron acceptor over NO_3^-.
277
278 *The relative abundances of the reductases could not explain the preference for N_2O over NO_3^-*
279 A proteomics analysis was done for strain HAMBI 2125. The abundance of NapA, NirK and NosZ
280 molecules, measured as intensities, were determined at different time points in cells sampled
281 during aerobic respiration (21% O_2), and during and after transition from 1% oxygen respiration
282 to denitrification (Fig. 4). The level of NorC molecules detected was two orders of magnitude

283 lower than those for the other reductases, suggesting that membrane-bound enzymes require a
284 different extraction protocol. Therefore, only values for the periplasmic reductases NapA, NirK
285 and NosZ were included here. The aerobic pre-incubation over several generations effectively
286 removed most denitrification reductases that may have lingered from earlier periods of anoxia,
287 seen from the signals from NapA and NirK being 293-585 times lower than those observed during
288 denitrification. Nos values were only 16-47 times lower, indicating low levels of constitutive
289 transcription of the *nos* gene and translation of the corresponding mRNA under aerobic
290 conditions. All three reductases increased in abundance during the O_2 depletion phase (blue) and
291 when O_2 approached depletion, the NapA/Nos and NapA/NirK ratios were 1.4±0.2 and 4.1±1.8
292 (sd, n=3). Interestingly, the NapA/Nos ratio was stable during the period of strong respiration of
293 exogenous N_2O, marked pink in Fig. 4, with values of 1.5± 0.3 and 1.2 ± 0.2, although practically
294 no NO_3^- reduction took place. The NapA/Nos ratio decreased to 0.7 during the phase of NO_3^-
295 reduction to N_2 (after depletion of exogenous N_2O). A similar pattern was found for the
296 NapA/NirK ratios, while the NosZ/NirK ratios stayed around 1.0 during the anaerobic phase.
297
298 *Growth rate and yield per mol electrons for aerobic and anaerobic respiration*
299 The experiment was designed to determine the growth rate and growth yield per mol electrons
300 for aerobic and anaerobic respiration (N_2O and NO_3^-), but also to inspect if cumulated electron
301 flow to the various electron acceptors could be used to predict cell density throughout a batch
302 incubation. The results summarized in Fig. 5 confirm that cumulated electron flow can be used
303 to predict increase in cell density (or dry weight, DW) throughout an incubation, provided that
304 the yield per electron to the various electron acceptors is known. The aerobic growth rate was

305 twice the anaerobic growth rate by N_2O respiration (0.063 and 0.031 h^{-1}). Growth from complete
306 denitrification (NO_3^- provided as e^- acceptor) was 0.024 h^{-1} (Fig. 5 A-C). The growth yield per mol
307 electrons was 7.17±0.38 g DW mol^{-1} e^- for aerobic respiration, 5.1±0.10 g DW mol^{-1} e^- from N_2O
308 respiration and 4.03±0.20 g DW mol^{-1} e^- for complete denitrification (NO_3^- to N_2) (Fig. 5D). In the
309 same experiment, we determined the DW per cell for cells grown by respiring O_2, N_2O and NO_3^-
310 (Fig. S7 B). Since the values for growth on the different electron acceptors were not significantly
311 different, they were regarded as replicates, giving an average cell DW of 615 ±54 fg (sd, n=12).
312

313 **Discussion**

314 The study comprised a set of taxonomically diverse *Bradyrhizobium* strains, as shown by the
315 phylogenetic tree (Figs 1, S1). This genus is commonly found among the most dominant
316 organisms in soil microbial communities (Delmont *et al*., 2012; Xu *at al*., 2014) and of large
317 environmental and economic value for their N_2-fixation ability in symbiosis with legumes. Based
318 on the MLSA analysis of four concatenated housekeeping genes (Fig. 1) the strains clustered in
319 eleven clades, covering various parts of the phylogenetic tree. Five strains in three clades did not
320 group with described *Bradyrhizobium* species, suggesting that three new species may be
321 delineated for these three clades. Our results from the denitrification analyses support other
322 studies showing that complete denitrification pathways are more common in the *B. japonicum*
323 supergroup than in other phylogenetic branches of *Bradyrhizobium* (Sameshima-Saito *et al.*, 2004**;**
324 Mania *et al*., 2020). The complete denitrifiers in the present study belonged to clusters related
325 to *B. shewense*, *B. ottawaense* and *B. guangxiense*, with the exception of one strain which
326 clustered with the distantly related *B. lablabi* (Fig. 1). Although this suggests that some taxonomic

327 groups of bradyrhizobia have higher frequency of complete denitrifiers than others, taxonomic
328 position cannot be used as an indicator of the denitrification end-product since even very closely
329 related strains may differ in this regard (Mania *et al.*, 2020).

330 Recent research has revealed several transcriptional and post-transcriptional mechanisms
331 that influence the amounts of intermediate products released from denitrifying organisms (Liu
332 *et al*., 2013; Torres *et al*., 2016; Lycus *et al*., 2018; Gaimster *et al*.,2019; Jiménez-Leiva *et al*., 2019).
333 Although of value by itself, such information may be anecdotal. To understand the environmental
334 relevance of a regulatory mechanism, it is important to know how widespread it is. We found the
335 same preference for N_2O over NO_3^- as electron acceptor in all strains with complete
336 denitrification, as did Mania *et al.* (2020) for a different set of isolates. This indicates a
337 phenomenon common to bradyrhizobia. In theory, it could be explained by lower numbers of
338 NapA molecules compared to NosZ molecules. The results by Mania *et al.* (2020) for strain AC
339 87j1, which is closely related to strain HAMBI 2125, could not disprove this, since transcription
340 analysis showed 5-8 times lower copy numbers of transcripts coding for NapA compared to NosZ.
341 This prompted us to perform a proteomics analysis in the present study. The results (Fig. 4)
342 provided clear evidence that the strong N_2O reduction was not due to higher abundance of NosZ
343 *vs* NapA, thus supporting the hypothesis by Mania *et al.* (2020) that the electron pathway to NosZ
344 is inherently more competitive than that to NapA.

345 Electrons from the quinol pool are channeled to Nap via the membrane-bound NapC, and to
346 Nos, Nor and Nir via the membrane-bound bc_1 complex and periplasmic cytochromes (Shapleigh,
347 2013). Most likely, the electron pathway to NosZ via bc_1 is inherently more competitive than that
348 to NapAB via NapC**,** plausibly due to a combination of stronger affinity for quinol and a higher k_{cat}

349 of bc_1 versus NapC. This implies a general mechanism which may apply not only to bradyrhizobia,
350 but possibly to all denitrifiers that carry Nap and Nos but lack the membrane-bound Nar.
351 Verifying this will require testing of a wide range of organisms. As a first step, we included in this
352 study a comparison of the denitrification kinetics of the bradyrhizobia with *P. denitrificans*, which
353 carries Nar in addition to Nap and Nos. The results supported our hypothesis by clearly
354 demonstrating that, while the *Bradyrhizobium* strains left NO_3^- untouched as long as exogenously
355 supplied N_2O was present (Figs 2A, S3, S4, S5), *P. denitrificans* reduced these electron acceptors
356 simultaneously (Fig. 2B). This suggests that the electron pathways from the quinol pool to NarG
357 via NarI and NarH and to NosZ via the bc_1 complex and cytochrome c compete equally well for
358 electrons, at least in *P. denitrificans*.

359 The proteomics analysis of HAMBI strain 2125 showed that NosZ was synthesized under fully
360 aeriated conditions, while NapA and NirK were not. Before sampling for proteomics analysis, the
361 cultures had been incubated in flasks with vigorous stirring for at least 10 generations to secure
362 that denitrification reductases produced during earlier exposure to denitrifying conditions were
363 diluted to near extinction in the cells. This was the case for NapA and NirK in the sample from
364 21% O_2 (Fig. 4). NosZ molecules were, however, approximately 10 times more abundant than
365 NapA and NirK during this phase, which suggests constitutive, albeit low, synthesis of NosZ. The
366 transcription analysis of strain AC87j1 reported by Mania *et al.* (2020) provides no clear
367 explanation to this, though. In the presence of 5 µM O_2 in the liquid, there were < 0.3 *nosZ* and
368 *nirK* transcripts $cell^{-1}$ with only slightly higher levels of *nosZ* than *nirK*. The *napA* transcription was
369 somewhat higher with 0.8 copies $cell^{-1}$. It is possible, still, that a low but steady production of Nos
370 takes place in these organisms irrespective of O_2 concentrations, in line with the higher β-

371 galactosidase activity observed for a *nos-lacZ* fusion of *B. japonicum* compared to a *nap-lacZ*
372 fusion (Bueno *et al.*, 2017; Torres *et al.*, 2017). This could be a strategy for cells to be prepared
373 for anaerobic conditions and avoid being entrapped in anoxia without enough energy to produce
374 the denitrification machinery (Lycus *et al.*, 2018). If so, it suggests that these bacteria may be
375 ready to reduce any N_2O produced by other organisms in their environment, thus acting as net
376 sinks for this greenhouse gas.

377 Seven strains lacked the last step of denitrification and thus had N_2O as end-product,
378 explained by the absence of the entire *nos* operon in all cases (Table S2). When exposed to
379 denitrifying conditions in the environment, such organisms will reduce all available N-oxides to
380 N_2O and thus act as net producers of this greenhouse gas. Three strains had NO as denitrification
381 end-product, but only HAMBI 2149 lacked the entire *nor* operon (Table S2). The other two strains,
382 HAMBI 2153 and 2299, contained *nor* operons but showed some sequence differences compared
383 to strains with functional NO reduction. Further investigations of the lacking NO reduction were,
384 however, beyond the scope of the present study. Organisms that produce NO but are incapable
385 of reducing it are apparently not uncommon (Casella *et al*., 2006; Falk *et al.*, 2010; Mania *et al.*,
386 2020). In the environment such organisms are most likely found in consortia with organisms that
387 express Nor or other NO-reducing enzymes.

388 The estimated growth yields were calculated based on the electron flow to the different
389 reductases (Fig. 5) and the proportions were expected to match that of the charge separations
390 per electron transport for the various respiratory pathways, as listed by (van Spanning *et al.*,
391 2007). The number of charge separations per 10 electrons ($q/10e^-$) are 50 for low affinity oxidase,
392 40 for high affinity oxidases, 30 for Nos alone, and 26 for the entire Nap, Nir, Nor, Nos

393 denitrification pathway (NO_3^- to N_2), which would a yield ratio of 100:60:52 for the three
394 pathways (O_2, N_2O, $NO_3 \rightarrow N_2$) if we assume that low affinity oxidases are used, and 100:75:65 for
395 high affinity oxidases. Our measured yields were 12, 8.5 and 6.7 $*10^{12}$ cells per mol electrons for
396 the three pathways, i.e. a yield ratio of 100:71:56, which agrees reasonably with that predicted
397 for high affinity oxidases.

398 The emerging evidence that bradyrhizobia with complete denitrification deplete N_2O in their
399 surroundings before reducing available NO_3^- is promising from an environmental point of view
400 since they have the potential to act as net sinks for N_2O produced by other organisms in their
401 vicinity. In legume fields, nodules and other N-rich organic material will be degraded, releasing
402 NH_4^+, which will rapidly be metabolized by nitrifying bacteria and archaea, producing NO_3^- while
403 consuming O_2. This will create optimal conditions for denitrification. Legume cropped fields
404 account for a significant share of the global N_2O emissions (Jensen *et al.*, 2012), and it is likely
405 that coupled nitrification-denitrification is a main cause (Bakken and Frostegård, 2017). One way
406 of mitigating these emissions is to enhance the number of efficient N_2O reducing bacteria in the
407 soil microbial community. Rhizobial inoculants are used since long to increase the yield of
408 leguminous crops and at the same time avoid the need for synthetic fertilizers. Different
409 combinations of rhizobial strain and legume cultivar may differ substantially in nitrogen fixation
410 effectiveness, which is also affected by environmental conditions (Woliy *et al.*, 2019; Lindström
411 and Mousavi, 2020), and large efforts are put into the development of new inoculants that are
412 compatible with various types of legumes as well as soil types and climates (Martínez *et al.*, 2016).
413 The present study shows that *Bradyrhizobium* strains also differ with respect to N_2O reduction,
414 and suggests that new inoculants should be selected among rhizobia that express Nos.

415

416 **Experimental Procedures**

417 *Bacterial strains*

418 The rhizobial isolates were obtained from various culture collections. Table 1 shows a list of host
419 plant and geographic origin of the strains used in the phylogenetic analysis (all listed isolates;
420 details see (Van Rossum *et al*., 1993; Van Rossum *et al*., 1994; Zhang *et al*., 1999; Chang *et al*.,
421 2011; Wang *et al*.,2013; Li *et al*., 2015; Degefu *et al*., 2017) and the strains analyzed for their
422 denitrification capacity (all except the four strains from Ethiopia earlier determined to have a
423 complete denitrification pathway (Mania *et al.,* 2020). Preparation of *Bradyrhizobium* cultures
424 and growth conditions followed Mania *et al.* (2020). All cultures were grown at 28 °C in Yeast
425 Mannitol Broth (YMB; 10 g l^{-1} D-mannitol, 0.5 g l^{-1} K_2HPO_4, 0.2 g l^{-1} $MgSO_4 \cdot 7H_2O$, 0.1 g l^{-1} NaCl and
426 0.5 g l^{-1} yeast extract, pH 7.0; Schwartz, 1972).

427

428 *Phylogenetic analyses*

429 DNA was extracted using QIAamp DNA Mini Kit (Qiagen). The genome sequences were obtained
430 from another ongoing project: (JGI Gold study ID: Gs0134353), and their Genome accession
431 numbers are listed in Table S3. Genome sequences were analyzed using RAST (Rapid Annotations
432 using Subsystems Technology). Whole-genome average nucleotide identity (ANI) comparisons
433 were done using FastANI v.0.1.2. A phylogenetic tree that included all HAMBI and CCBAU strains
434 from this study (Table 1), as well as the Ethiopian strains AC70c, AC86d2, AC87j1 and AC101b and
435 the type strain of all species of the genus *Bradyrhizobium* (February 2020,
436 http://www.bacterio.net/bradyrhizobium.html), was constructed based on multilocus sequence

437 analysis (MLSA) of the four housekeeping genes *atpD* (ATP synthase F1, beta
438 subunit), *glnII* (glutamine synthetase type II), *recA* (recombinase A), *rpoB* (RNA polymerase, beta
439 subunit). The sequences from all HAMBI strains used in the MLSA analysis were obtained from
440 the present study. Amplicons of *rpoB* and *atpD* of the Ethiopian strains AC70c, AC86d2 and
441 AC101b and *recA* from AC70c were Sanger sequenced. For primers and PCR conditions, see Table
442 S4. All other sequences were obtained from GenBank (http://www.ncbi.nlm.nih.gov/genbank).
443 The GeneBank accession numbers for all housekeeping genes used are listed in Table S5. The
444 gene sequences were aligned by ClustalW (Larkin *et al.*, 2007) in Bioedit v7.0.5.3 (Hall, 1999), and
445 the alignments were edited manually. The best-fit models of nucleotide substitution were
446 selected based on Akaike information criterion (AIC) applying MEGA7 (Kumar *et al.*, 2016).
447 The Bayesian phylogenetic analyses of the concatenated loci (*atpD-recA-glnII-rpoB*) of 78
448 *Bradyrhizobium* strains were performed using the algorithm Metropolis coupled Markov chain
449 Monte Carlo (MCMCMC) twice for ten million generations using MrBayes v3.2.7a program
450 (Ronquist *et al.*, 2012). *Neorhizobium galegae* was used to root the tree. The general time
451 reversible plus gamma distribution plus invariable sites (GTR + G + I) was chosen as the best-fit
452 model of phylogenetic analyses of the four partition of the concatenated dataset (*atpD-glnII-*
453 *recA-rpoB*). The algorithms were analyzed using Tracer v1.7 (Rambaut *et al.*, 2018), and the
454 phylogenetic trees were visualized by Figtree v1.4.3 (https://beast.community/figtree). For
455 comparison with the MLSA tree based on four housekeeping genes, a phylogenetic tree of all the
456 HAMBI test strains listed in Table S2 was constructed using the Genome Taxonomy Database
457 Toolkit (GTDB-Tk) v0.3.2, which is based on a phylogeny inferred from the concatenation of 120
458 ubiquitous, single-copy proteins (Chaumeil *et al*., 2020).

459

460 *Denitrification end products and gas kinetics analyses*

461 Prior to these experiments the cultures were streaked for purity and single colonies were picked
462 and checked for possible contaminating bacteria by sequencing of the 16S rRNA genes (for
463 primers and PCR conditions see Table S4). Pure cultures were preserved as in glycerol (15%) at -
464 80 °C. Cultures were raised from these frozen stocks in stirred batches of 50 ml YMB
465 supplemented with filter sterilized KNO_3 and/or KNO_2 solutions. The flasks were sealed with
466 sterilized, gas tight butyl rubber septa (Matrix AS, Norway). Air was removed by applying vacuum
467 for 6 x 360 s, followed by 30 s He-filling. The desired amount of O_2 and/or N_2O was injected into
468 the headspace, and the over-pressure released (Molstad *et al.*, 2007). Denitrification kinetics of
469 *Bradyrhizobium* strains with complete denitrification pathways were compared to the model
470 bacterium *Paracoccus denitrificans* PD1222, which was grown under the same conditions as the
471 *Bradyrhizobium* strains, except that Sistrom´s medium supplemented with 2 mM KNO_3 was used
472 (Sistrom, 1962; Bergaust *et al.*, 2010).

473 Denitrification end-products were determined for all strains as described previously (Lycus *et*
474 *al.*, 2017). Detailed gas kinetics were measured following Mania *et al*. (2020). Pre-cultures were
475 added to incubation flasks (n=3) supplied with 1 mM initial KNO_3 and, when indicated, also with
476 0.5 mM KNO_2. Unless stated otherwise, 0.7 mL O_2 (1 vol% in headspace) and 0.7 ml N_2O
477 (approximately 50 µmol N flask^{-1}) were added to the headspace at the start of the experiment (0
478 hpi, hours post inoculation). For the determination of end-products, the amounts of O_2, NO, N_2O
479 and N_2 in the headspace were measured at the start and after 10 days of incubation.

480 All strains with a complete denitrification pathway according to the end-point analysis, as
481 well as all HAMBI strains that had NO as end-product, were investigated further by analyzing gas
482 kinetics in response to oxygen depletion. To secure an inoculum in which any previously
483 synthesized denitrification enzymes had been diluted out by aerobic growth, all cultures were
484 precultured aerobically for at least 6-8 generations. This was done in uncapped flasks covered
485 with aluminum foil (to allow oxygen transport), with vigorous stirring (600 rpm) at 28 ˚C. To
486 further ensure the absence of hypoxia, the cultures were transferred to new flasks before the
487 OD_{600} reached 0.3. Portions of the precultures were inoculated into 120 ml flasks containing 50
488 ml YMB supplemented with 1, 2 or 3 mM KNO_3 and with He, O_2 and N_2O in headspace as
489 described above for the end-product measurements. The flasks were placed in a robotized
490 incubation system that frequently measured O_2, NO, N_2O and N_2 in headspace (Molstad *et al.*,
491 2007; Molstad *et al.*, 2016). Leakage and sampling losses were taken into account when
492 calculating the rates of production/consumption of each gas, see Molstad *et al*. (2007) for details.
493 Earlier experiments determined that no gas production (NO, N_2O or N_2) took place from chemical
494 reactions between of NO_2^- and the medium under the conditions used (Mania *et al.*, 2020).
495

496 *Nitrite measurements*

497 Samples for NO_2^- measurements (0.1-1.0 ml) were taken manually from the liquid phase through
498 the rubber septum of the flasks using a sterile syringe. NO_2^- concentrations were determined
499 immediately after each sampling by drawing a 10 µL liquid sample which was injected into a
500 purging device containing 50% acetic acid with 1% (w/v) NaI (at room temperature), by which
501 NO_2^- is reduced instantaneously to NO (Cox, 1980; MacArthur *et al.*, 2007). The quantities of

502 resultant NO were measured by chemiluminescence using a NO analyser (Sievers NOA™ 280i, GE
503 Analytical Instruments). The system was calibrated by injecting standards. Sampling for NO_2^-
504 measurements was done as frequently as the gas sampling.
505
506 *Proteomics*
507 Relative quantification of the denitrification reductases was done for the strain *Bradyrhizobium*
508 sp. HAMBI 2125, chosen as a representative for the complete denitrifiers (Fig. 1), which all
509 showed the same preference for N_2O over NO_3^- reduction (Figs 2A, S3, S4, S5). Cells were first
510 raised from frozen stock under strictly aerobic conditions as explained above. As the aerobic
511 preculture reached OD_{600} = 0.05 ($2.9*10^7$ cells ml^{-1}), it was used to inoculate 18 flasks (1 ml
512 inoculum $flask^{-1}$) containing YMB with 1 mM NO_3^- and with 1 ml N_2O (approximately 80 µmol
513 N_2O-N $flask^{-1}$) and 1 % O_2 in headspace. Samples for protein analysis were taken i) from the
514 aerobic inoculum; ii) just before transition to anaerobic respiration (22 hpi, when O_2 reached ~4.6
515 µM); iii) during the period of rapid reduction of exogenous N_2O (27 and 32 hpi); and iv) during
516 the period of NO_3^- reduction to N_2 (36 hpi). Three replicate flasks were harvested at each time
517 point. Gas kinetics, NO_2^- concentrations and sampling times for proteomics are shown in Fig. S8.
518 After measuring the OD_{600}, the samples were centrifuged (10 000 g, 4 °C, 10 min) and the cell
519 pellets were stored at -20 °C for protein extraction. In addition, we harvested and froze cells from
520 the aerobic preculture.
521 To extract the proteins, the cell pellets were thawed, resuspended in lysis buffer (20 mM Tris-
522 HCl pH8, 0.1 % v/v Triton X-100, 200 mM NaCl, 1 mM DTT) and treated with 3x45 s bead beating
523 with glass beads (particle size ⩽106 µm Sigma) at maximum power and cooling on ice between

524 the cycles (MP Biomedicals™ FastPrep- 24™, Thermo Fischer Scientific Inc). Cell debris was
525 removed by centrifugation (10 000 g; 5 min) and the supernatant, containing water soluble
526 proteins, was used for proteomic analysis based on Orbitrap-MS as described before (Conthe *et*
527 *al.*, 2019). To quantify the denitrification reductases we calculated the fraction of the individual
528 enzymes as percentages of the sum of all LFQ (label-free quantitation of proteins) abundances
529 for each time point.
530
531 *Determinations of growth and yield*
532 Aerobic and anaerobic growth was investigated in detail for *Bradyrhizobium* sp. HAMBI 2125 to
533 determine the growth yield per mol electrons transferred to O_2, N_2O, and to the entire
534 denitrification pathway. Four treatments were compared: 1) 7% O_2 in headspace; 2) 0% O_2, 4 mM
535 NO_3^-; 3) 0% O_2 and 10 ml N_2O; 4) 7% O_2, 4 mM NO_3^- and 10 ml N_2O. All treatments had an excess
536 of electron donor (>70 times more electrons than needed to reduce the electron acceptor). Pre-
537 cultures were started from single colonies and grown in YMB under fully oxic conditions (21% O_2)
538 for inoculation of the aerobic batch cultures (treatments 1 and 4), and under anoxic conditions
539 for inoculation of the anaerobic batches (treatments 2 and 3). The OD_{600} of the aerobic pre-
540 cultures was kept < 0.3 by regularly inoculating portions of the culture into flasks with fresh
541 medium. There were 6 replicate flasks for each treatment. Liquid samples were taken from three
542 of them every 6 h (0.85 ml) for growth measurements (OD_{600}). The three other replicates were
543 only monitored for gas kinetics and were then used to measure final cell dry weight, to assess
544 the growth yield per mol electrons to O_2 and N-oxides. For determinination of cell dry weight,
545 cultures were centrifuged, washed twice in distilled water and dried at 100 ^oC before weighing.

546 Cell numbers were determined by microscopic counts at selected sampling times, which gave a
547 conversion factor of $5.8*10^8$ cells ml^{-1} * OD_{600}^{-1}. The estimated yield from growth on O_2, N_2O and
548 NO_3^- was 12.0, 8.5 and 6.7 E12 cells mol^{-1} electrons, respectively (Figs 5, S7). The yields were used
549 to calculate cell density throughout the incubations, enabling the calculation of cell specific rates
550 of electron flows to the various electron acceptors, for details see Fig. S7.
551

552 **Acknowledgements**

553 This project was supported by Kingenta Ecological Engineering Co., LTD. Yuan Gao is grateful to
554 the China Scholarship Council (CSC) for financial support. We thank Dr. Xinghua Sui from China
555 Agricultural University for providing seven of the *Bradyrhziobium* strains.

556

557 **Ethics declarations**

558 The authors declare that they have no conflict of interest.

559

560 **References**

561 Akiyama, H., Hoshino, Y.T., Itakura, M., Shimomura, Y., Wang, Y., Yamamoto, A., *et al*. (2016) Mitigation
562 of soil N_2O emission by inoculation with a mixed culture of indigenous *Bradyrhizobium diazoefficiens*. *Sci*
563 *Rep* **6**: 32869.
564 Arya, S.S., Salve, A.R., Chauhan, S. (2016) Peanuts as functional food: a review. *J Food Sci Technol* **53**: 31–
565 41.
566 Avontuur, J.R., Palmer, M., Beukes, C.W., Chan, W.Y., Coetzee, M.P.A., Blom, J., *et al*. (2019) Genome-
567 informed *Bradyrhizobium* taxonomy: where to from here? *Syst Appl Microbiol* **42**: 427-439.

568 Bakken, L.R., Frostegård, Å. (2017) Sources and sinks for N_2O, can microbiologist help to mitigate N_2O
569 emissions? *Environ Microbiol* **19**: 4801-4805.
570 Bedmar, E.J., Robles, E.F., Delgado, M.J. (2005) The complete denitrification pathway of the symbiotic,
571 nitrogen-fixing bacterium *Bradyrhizobium japonicum*. *Biochem Soc Trans* **33**: 141–144.
572 Bergaust, L., Mao, Y., Bakken, L.R., Frostegård, Å. (2010) Denitrification response patterns during the
573 transition to anoxic respiration and posttranscriptional effects of suboptimal ph on nitrogen oxide
574 reductase in *Paracoccus denitrificans*. *Appl Environ Microbiol* **76**: 6387–6396.
575 Berks, B.C., Ferguson, S.J., Moir, J.W.B., Richardson, D.J. (1995) Enzymes and associated electron
576 transport systems that catalyse the respiratory reduction of nitrogen oxides and oxyanions. *Biochim*
577 *Biophys Acta* **1232**: 97–173.
578 Bueno, E., Robles, E.F., Torres, M.J., Krell, T., Bedmar, E.J., Delgado, M.J., *et al*. (2017) Disparate
579 response to microoxia and nitrogen oxides of the *Bradyrhizobium japonicum napEDABC*, *nirK* and
580 *norCBQD* denitrification genes. *Nitric Oxide* **68**: 137–149.
581 Casella, S., Shapleigh, J.P., Toffanin, A., Basaglia, M. (2006) Investigation into the role of the truncated
582 denitrification chain in *Rhizobium sullae* strain HCNT1. *Biochem Soc Trans* **34**: 130-132.
583 Chang, Y.L., Wang, E.T., Sui, X.H., Zhang, X.X., Chen, W.X. (2011) Molecular diversity and phylogeny of
584 rhizobia associated with *Lablab purpureus* (Linn.) grown in Southen China. *Syst Appl Microbiol* **34**: 276-
585 284.
586 Chaumeil, P.A., Mussig, A.J., Hugenholtz, P., Parks, D.H. (2020) GTDB-Tk: a toolkit to classify genomes
587 with the Genome Taxonomy Database. *Bioinformatics* **36**: 1925-1927.
588 Conthe, M., Lycus, P., Arntzen, M.Ø., Ramos da Silva, A., Frostegård, Å., Bakken, L.R., *et al*. (2019)
589 Denitrification as an N_2O sink. *Water Res* **151**: 381–387.
590 Cox, R.D. (1980) Determination of nitrate and nitrite at the parts per billion level by chemiluminescence.
591 *Anal Chem* **52**: 332–335.

592 Davidson, E.A., Kanter, D. (2014) Inventories and scenarios of nitrous oxide emissions. *Environ Res Lett*
593 **9**: 105012.
594 Degefu, T., Wolde-meskel, E., Woliy, K., Frostegård, Å. (2017) Phylogenetically diverse groups of
595 *Bradyrhizobium* isolated from nodules of tree and annual legume species growing in Ethiopia. *Syst Appl*
596 *Microbiol* **40**: 205-214.
597 Delgado, M.J., Bonnard, N., Tresierra-Ayala, A., Bedmar, E.J., Müller, P. (2003) The *Bradyrhizobium*
598 *japonicum napEDABC* genes encoding the periplasmic nitrate reductase are essential for nitrate
599 respiration. *Microbiology* **149**: 3395–3403.
600 Delmont, T.O., Prestat, E., Keegan, K.P., Faubladier, M., Robe, P., Clark, I.M., *et al*. (2012) Structure,
601 fluctuation and magnitude of a natural grassland soil metagenome. *ISME J* **6**: 1677-1687.
602 Falk, S., Liu, B., Braker, G. (2010) Isolation, genetic and functional characterization of novel soil *nirK*-type
603 denitrifiers. *Syst Appl Microbiol* **33**: 337–347.
604 Gaimster, H., Hews, C.L., Griffiths, R., Soriano-Laguna, M.J., Alston, M., Richardson, D.J., *et al*. (2019) A
605 central small RNA regulatory circuit controlling bacterial denitrification and N_2O emissions. *mBio* **10**:
606 e01165-19.
607 Hall, T.A. (1999) BioEdit: a user-friendly biological sequence alignment editor and analysis program for
608 Windows 95/98/NT. *Nucleic Acids Symposium Series* **41***:* 95–98.
609 Hénault, C., Revellin, C. (2011) Inoculants of leguminous crops for mitigating soil emissions of the
610 greenhouse gas nitrous oxide. *Plant Soil* **346**: 289-296.
611 Itakura, M., Uchida, Y., Akiyama, H., Hoshino, Y.T., Shimomura, Y., Morimoto, S., *et al*. (2013) Mitigation
612 of nitrous oxide emissions from soils by *Bradyrhizobium japonicum* inoculation. *Nat Clim Chang* **3**: 208–
613 212.
614 Jensen, E.S., Peoples, M.B., Boddey, R.M., Gresshoff, P.M., Hauggaard-Nielsen, H., Alves, J.R., *et al*.
615 (2012) Legumes for mitigation of climate change and the provision of feedstock for biofuels and

616 biorefineries. A review. *Agron Sustain Dev*. **32**: 329–364.

617 Jiménez-Leiva, A., Cabrera, J.J., Bueno, E., Torres, M.J., Salazar, S., Bedmar, E.J., *et al*. (2019) Expanding
618 the Regulon of the *Bradyrhizobium diazoefficiens* NnrR Transcription Factor: New Insights Into the
619 Denitrification Pathway. *Front Microbiol* **10**: 1926.

620 Kumar, S., Stecher, G., Tamura, K. (2016) MEGA7: Molecular Evolutionary Genetics Analysis Version 7.0
621 for Bigger Datasets. *Mol Biol Evol* **33**: 1870–1874.

622 Larkin, M.A., Blackshields, G., Brown, N.P., Chenna, R., Mcgettigan, P.A., McWilliam, H., *et al*. (2007)
623 Clustal W and Clustal X version 2.0. *Bioinformatics* **23**: 2947–2948.

624 Li, Y.H., Wang, R., Zhang, X.X., Young, P.W., Wang, E.T., Sui, X.H., *et al*. (2015) *Bradyrhizobium*
625 *guangdongense* sp. nov. and *Bradyrhizobium guangxiense* sp.nov., isolated from effectvie nodules of
626 peanut. *Int J Syst Evol Microbiol* **65**: 4655-4661.

627 Lindström, K., Mousavi, S.A. (2020) Effectiveness of nitrogen fixation in rhizobia. *Microb Biotechnol* **13**:
628 1314-1335.

629 Liu, B., Mao, Y., Bergaust, L., Bakken, L.R., Frostegård, Å. (2013) Strains in the genus *Thauera* exhibit
630 remarkably different denitrification regulatory phenotypes. *Environ Microbiol* **15**: 2816–2828.

631 Lycus, P., Bøthun, K.L., Bergaust, L., Shapleigh, J.P., Bakken, L.R., Frostegård, Å. (2017) Phenotypic and
632 genotypic richness of denitrifiers revealed by a novel isolation strategy. *ISME J* **11**: 2219–2232.

633 Lycus, P., Soriano-Laguna, M.J., Kjos, M., Richardson, D.J., Gates, A.J., Milligan, D.A., *et al*. (2018) A bet-
634 hedging strategy for denitrifying bacteria curtails their release of N_2O. *Proc Natl Acad Sci* **115**: 11820–
635 11825.

636 MacArthur, P.H., Shiva, S., Gladwin, M.T. (2007) Measurement of circulating nitrite and S-nitrosothiols
637 by reductive chemiluminescence. *J Chromatogr B* **851**: 93–105.

638 Mania, D., Woliy, K., Degefu, T., Frostegård, Å. (2020) A common mechanism for efficient N_2O reduction
639 in diverse isolates of nodule-forming bradyrhizobia. *Environ Microbiol* **22**: 17–31.

640 Martínez, J., Negrete-Yankelevich, S., Godinez, L.G., Reyes, J., Esposti, M.D., Martínez Romero, E. (2016)
641 Short-Term Evolution of Rhizobial Strains Toward Sustainability in Agriculture. In *Microbial Models: From*
642 *Environmental to Industrial Sustainability*. Springer: Singapore, pp. 277–292.
643 Mesa, S., Velasco, L., Manzanera, M.E., Delgado, M.J., Bedmar, E.J. (2002) Characterization of the
644 *norCBQD* genes, encoding nitric oxide reductase, in the nitrogen fixing bacterium *Bradyrhizobium*
645 *japonicum*. *Microbiology* **148**: 3553–3560.
646 Molstad, L., Dörsch, P., Bakken, L.R. (2016) Improved robotized incubation system for gas kinetics in
647 batch cultures. *ResearchGate*. https://doi.org/10.13140/RG.2.2.30688.07680.
648 Molstad, L., Dörsch, P., Bakken, L.R. (2007) Robotized incubation system for monitoring gases (O_2, NO,
649 N_2O N_2) in denitrifying cultures. *J Microbiol Methods* **71**: 202–211.
650 Obando, M., Correa-Galeote, D., Castellano-Hinojosa, A., Gualpa, J., Hidalgo, A., Alché, J.D., *et al*. (2019)
651 Analysis of the denitrification pathway and greenhouse gases emissions in *Bradyrhizobium* sp. strains
652 used as biofertilizers in South America. *J Appl Microbiol* **127**: 739–749.
653 Rambaut, A., Drummond, A.J., Xie, D., Baele, G., Suchard, M.A. (2018) Posterior summarization in
654 Bayesian phylogenetics using Tracer 1.7. *Syst Biol* **67**: 901–904.
655 Reay, D.S., Davidson, E.A., Smith, K.A., Smith, P., Melillo, J.M., Dentener, F., *et al*. (2012) Global
656 agriculture and nitrous oxide emissions. *Nat Clim Chang* **2**: 410–416.
657 Richardson, D.J. (2000) Bacterial respiration: a flexible process for a changing environment. *Microbiology*
658 **146**: 551–571.
659 Richardson, D.J., Berks, B.C., Russell, D.A., Spiro, S., Taylor, C.J. (2001) Functional, biochemical and
660 genetic diversity of prokaryotic nitrate reductases. *Cell Mol Life Sci* **58**: 165–178.
661 Rogelj, J., Shindell, D., Jiang, K., Fifita, S., Forster, P., Ginzburg, V., *et al*. (2018) Mitigation pathways
662 compatible with 1.5 °C in the context of sustainable development. In, Masson-Delmotte V, Zhai P,
663 Pörtner HO, Roberts D, Skea J, Shukla PR, et al. (eds). *Global Warming of 1.5 °C. An IPCC Special Report*

on the impacts of global warming of 1.5°C above pre-industrial levels and related global greenhouse gas emission pathways, in the context of strengthening the global response to the threat ofclimate change, sustainable development, and efforts to eradicate poverty; https://www.ipcc.ch/site/assets/uploads/sites/2/2019/02/SR15_Chapter2_Low_Res.pdf.

Ronquist, F., Teslenko, M., Van Der Mark, P., Ayres, D.L., Darling, A., Höhna, S., *et al*. (2012) Mrbayes 3.2: Efficient bayesian phylogenetic inference and model choice across a large model space. *Syst Biol* **61**: 539–542.

Sameshima-Saito, R., Chiba, K., Minamisawa, K. (2004) New method of denitrification analysis of *Bradyrhizobium* field isolates by gas chromatographic determination of ^{15}N-labeled N_2. *Appl Environ Microbiol* **70**: 2886–2891.

Sánchez, C., Minamisawa, K. (2018) Redundant roles of *Bradyrhizobium oligotrophicum* Cu-type (NirK) and cd1-type (NirS) nitrite reductase genes under denitrifying conditions. *FEMS Microbiol Lett* **365**: fny015.

Santos, M.S., Nogueira, M.A., Hungria, M. (2019) Microbial inoculants: reviewing the past, discussing the present and previewing an outstanding future for the use of beneficial bacteria in agriculture. *AMB Expr* **9**: 205.

Schlesinger, W.H. (2009) On the fate of anthropogenic nitrogen. *Proc Natl Acad Sci* **106**: 203–208.

Schwartz, W. (1972) Vincent, J.M, a manual for the practical study of the root-nodule bacteria (IBP Handbuch no. 15 des international biology program, London). XI u. 164 S., 10 Abb., 17 tab., 7 Taf. Oxford-Edinburgh 1970: Blackwell scientific Publ.,45 s. *Z Allg Mikrobiol* **12**: 1521–4028.

Shapleigh, J.P. (2013) The prokaryotes: Prokaryotic physiology and biochemistry. In Rosenberg E, DeLong EF, Lory S, Stackebrandt E, Thompson F (eds). *The prokaryotes.* Springer: Berlin Heidelberg, pp 405–425.

Sistrom, W.R. (1962) The kinetics of the synthesis of photopigments in Rhodopseudomonas spheroides. *J Gen Microbiol* **28**: 607–616.

688 Thompson, R.L., Lassaletta, L., Patra, P.K., Wilson, C., Wells, K.C., Gressent, A., *et al*. (2019) Acceleration
689 of global N_2O emissions seen from two decades of atmospheric inversion. *Nat Clim Chang* **9**: 993–998.
690 Thomson, A.J., Giannopoulos, G., Pretty, J., Baggs, E.M., Richardson, D.J. (2012) Biological sources and
691 sinks of nitrous oxide and strategies to mitigate emissions. *Philos Trans R Soc B.* **367**: 1157-1168.
692 Thrall, P.H., Laine, A-L., Broadhurst, L.M., Bagnall, D.J., Brockwell, J. (2011) Symbiotic effectiveness of
693 rhizobial mutualists varies in interactions with native Australian legume genera. *PLoS ONE* **6**: e23545.
694 Tian, H., Xu, R., Canadell, J.G., Thompson, R.L., Winiwarter, W., Suntharalingam, P., *et al*. (2020) A
695 comprehensive quantification of global nitrous oxide surces and sinks. *Nature* **586**: 248-256.
696 Torres, M.J., Bueno, E., Jiménez-Leiva, A., Cabrera, J.J., Bedmar, E.J., Mesa, S., *et al*. (2017) $FixK_2$ Is the
697 Main Transcriptional Activator of *Bradyrhizobium diazoefficiens nosRZDYFLX* Genes in Response to Low
698 Oxygen. *Front Microbiol* **8**: 1621.
699 Torres, M.J., Simon, J., Rowley, G., Bedmar, E.J., Richardson, D.J., Gates, A.J., *et al*. (2016) Nitrous oxide
700 metabolism in nitrate-reducing bacteria: physiology and regulatory mechanisms. In: Poole RK (eds).
701 *Advances in microbial physiology*, first edition. Elsevier, pp 353-432.
702 Van Rossum, D., Muyotcha, A., Van Verseveld, H.W., Stouthamer, A.H., Boogerd, F.C. (1993) Effects of
703 *Bradyrhizobium* strain and host genotype, nodule dry weight and leaf aera on groundnut *(Arachis*
704 *hypogaea L. ssp. fastigiata)* yield. *Plant and Soil* **154**: 279-288.
705 Van Rossum, D., Muyotcha, A., Van Verseveld, H.W., Stouthamer, A.H., Boogerd, F.C. (1994) Siderophore
706 production by *Bradyrhizobium* spp. Strains nodulating groundnut. *Plant and soil* **163**: 177-187.
707 Van Spanning, R., Richardson, D., Ferguson, S. (2007) Introduction to the biochemistry and molecular
708 biology of denitrification. In: Bothe H,Ferguson SJ, Newton WE (eds). *Biology of the nitrogen cylce*.
709 Elsevier: Amsterdam, The Netherlands, pp 3–21.
710 Velasco, L., Mesa, S., Delgado, M.J., Bedmar, E.J. (2001) Characterization of the *nirK* gene encoding the
711 respiratory, Cu-containing nitrite reductase of *Bradyrhizobium japonicum*. *Biochim Biophys Acta* **1521**:

130–134.

Velasco, L., Mesa, S., Xu, C., Delgado, M.J., Bedmar, E.J. (2004) Molecular characterization of *nosRZDFYLX* genes coding for denitrifying nitrous oxide reductase of *Bradyrhizobium japonicum*. *Antonie Van Leeuwenhoek* **85**: 229–235.

Wang, R., Chang, Y.L., Zheng, W.T., Zhang, D., Zhang, X.X., Sui, X.H., *et al*. (2013) *Bradyrhizobium arachidis* sp. Nov., isolated from effective nodules of Arachis hypogaea grown in China. *Syst Appl Microbiol* **36**: 101-105.

Winiwarter, W., Höglund-Isaksson, L., Klimont, Z., Schöpp, W., Amann, M. (2018) Technical opportunities to reduce global anthropogenic emissions of nitrous oxide. *Environ Res Lett* **13**: 014011.

Woliy, K., Degefu, T., Frostegård, Å. (2019) Host Range and Symbiotic Effectiveness of N_2O Reducing *Bradyrhizobium* Strains. *Front Microbiol* **10**: 2746.

Xu, Z.F., Hansen, M.A., Hansen, L.H., Jacquiod, S., Sørensen, S.J. (2014) Bioinformatic Approaches Reveal Metagenomic Characterization of Soil Microbial Community. *PLoS ONE* **9**: e93445.

Zhang, L., Wüst, A., Prasser, B., Müller, C., Einsle, O. (2019) Functional assembly of nitrous oxide reductase provides insights into copper site maturation. *Proc Natl Acad Sci* **116**: 12822–12827.

Zhang, X.P., Nick, G., Kaijalainen, S., Terefework, Z., Paulin, L., Tighe, S.W., *et al*. (1999) Phylogeny and Diversity of *Bradyrhizobium Strains* isoalted from the Root Nodules of Peanut *(Arachis hypogaea)* in Sichuan, China. *Syst Appl Microbiol* **22**: 378-386.

Zilli, .JÉ., Alves, B.J.R., Rouws, L.F.M., Simões-Araujo, J.L., de Barros Soares, L.H., Cassán, F., *et al*. (2019) The importance of denitrification performed by nitrogen-fixing bacteria used as inoculants in South America. *Plant Soil* **451**: 5-24.

Zumft, W.G. (1997) Cell biology and molecular basis of denitrification. *Microbiol Mol Biol Rev* **61**: 533–616.

736 **Table and Figure legends**

737 **Table 1**. Strains used in the current study. All listed strains were included in the MLSA-based phylogenetic
738 analysis (Fig. 1). The strains above the dashed line were also examined in the present study with regard
739 to their denitrification phenotypes. Strains AC 70c, AC 86d2, AC 86j1 and AC 101b were not examined for
740 denitrification since this was reported elsewhere (Mania *et al*., 2020).

741

742 **Fig. 1.** Phylogenetic tree of four concatenated housekeeping genes (*atpD- glnII- recA- rpoB*) from 78
743 *Bradyrhizobium* strains constructed based on a Bayesian inference analysis. Only the posterior
744 probabilities ≥0.95 are shown in the tree. The genus name *Bradyrhizobium* is abbreviated as *B*., and a "T"
745 at the end of each strain code shows the type strains. In cases where two or more isolates showed high
746 whole genome sequence similarity (>99 %) based on pairwise comparison of Average Nucleotide Identity
747 (ANI) (see Table S1), only one representative is shown in this tree. Colors indicate denitrification end-
748 products. A sequence analysis of the genes in the respective denitrification gene operons showed good
749 correspondence between genetic set-up and denitrification end products (Table S2). The only exception
750 was HAMBI 2299, which had a complete *nor* operon but did not reduce NO. Another non-NO reducing
751 strain, HAMBI 2153, lacked two genes in the *nor* operon.

752

753 **Fig. 2.** Competition for electrons between N_2O- and NO_3^- reductase; comparison of Nap- and Nar-carrying
754 organisms. Gas kinetics and corresponding electron flow to oxidases (aerobic respiration) and to the
755 different N-reductases (denitrification) in batch cultures of *Bradyrhizobium* strain HAMBI 2125 and
756 *Paracoccus denitrificans*. Both organisms perform complete denitrification but *Bradyrhizobium* (A, C)
757 carries only the periplasmic NapA for dissimilatory NO_3^- reduction while *P. denitrificans* (B, D) carries both
758 NapA and the membrane-bond NarG. The top panels (A, B) show the measured amounts of NO_2^-, NO, N_2O
759 and N_2 per flask, and the concentration of O_2 in the liquid. Note that the small but significant decrease in
760 N_2O during the aerobic phase was caused by sampling losses, not by N_2O reduction or other reactions, as
761 explained in Fig. S6. Background colors indicate the dominating respiratory activity. Blue: O_2 respiration;
762 Pink: N_2O respiration; Green: Complete denitrification (NO_3^- to N_2). The bottom panels (C, D) show the
763 calculated cell specific rates of electron flow (fmol $cell^{-1}$ h^{-1}) to the terminal oxidases (V_{eO2}) and to the four
764 reductases ($V_{eNar/Nap}$, V_{eNir}, V_{eNor} and V_{eNos}). V_{eNir} and V_{eNor} were practically identical throughout (NO
765 remained very low), thus indistinguishable in the panels. Strain HAMBI 2125 was incubated in 4 replicate
766 flasks with YMB supplemented with 1 mM KNO_3, of which only one is shown here (gas- and NO_2^- kinetics

767 of replicate flasks are shown in Fig. S3). *P. denitrificans* was incubated in 50 ml Sistrom's medium with 2
768 mM KNO_3 (n=7, bars show standard errors). At the start of the incubation, all flasks contained ~1% O_2 in
769 the headspace (~10 µM in liquid) and ~ 1.2 ml N_2O (~90 µmol N_2O-N). $V_{eNar/Nap}$ and V_{eNir} represent rates
770 of electron transport to NO_3^- and NO_2^-, respectively (via NapA and NirK for *Bradyrhziobium* and via
771 NarG+Nap and NirS for *P. denitrificans*).

772

773 **Fig. 3**. Effect of injecting N_2O to an actively denitrifying culture. Gas kinetics for *Bradyrhizobium* strain
774 HAMBI 2125 during and after transition from aerobic respiration to N-oxide respiration. Triplicate cultures
775 were incubated in YMB medium supplemented with 2 mM KNO_3 and with 0.7 ml O_2 in the headspace
776 (around 10 µM O_2 in the medium). Approximately 4 ml N_2O (~300 µmol N_2O-N) were injected at 32 hpi,
777 indicated by the arrow, into actively denitrifying cultures respiring NO_3^-. Bars show standard errors (n=3).

778

779 **Fig. 4.** Abundance of denitrification reductases during and after transition from aerobic to anaerobic
780 respiration. The abundances of Nap, NirK and Nos were determined by proteomics and calculated as
781 percentages of the sum of all LFQ (label-free quantitation of proteins) abundances for each time point.
782 The first samples were taken from triplicate flasks of *Bradyrhizobium* strain HAMBI 2125 growing under
783 fully oxic conditions (21% O_2). Subsamples from these precultures were inoculated into flasks with 1% O_2,
784 and samples for proteomics were taken when the cultures approached O_2 depletion ([O_2] = 5.8±0.2 µM)
785 and during the anaerobic respiration. Concentrations of O_2 (grey shading) and N_2O (-Δ-) are schematically
786 indicated here to illustrate the time of their depletion; for actual values of [O_2] [N_2O], [N_2] and [NO_2^-], see
787 Fig. S8. Background colors indicate the dominating respiratory activity. Blue: O_2 respiration; Pink: N_2O
788 respiration; Green: Complete denitrification (NO_3^- to N_2). Bars show standard deviation (n=3).

789

790 **Fig. 5.** Growth and yield of *Bradyrhizobium* strain HAMBI 2125 when incubated in YMB at 28 °C and
791 provided with O_2, N_2O or NO_3^- as electron acceptor. All relevant gases were measured frequently using a
792 robotized system. Panels A-C show estimated g dry weight (DW) flask^{-1} throughout the incubations either
793 calculated from measured OD_{600} (□) using the factor 0.374 mg dry weight ml^{-1} OD_{600}^{-1} (Fig. S7) or calculated
794 from the measured cumulated electron flow (solid line) using measured yields per mol e^- in panel D. The
795 specific growth rates (µ) were determined by regression of ln(OD_{600}) against time during the period of
796 exponential growth. Panel A. Growth using O_2 as sole electron acceptor (initial amount 180 µmol flask^{-1}).

797 Panel B. Growth using N_2O as sole electron acceptor (initial amount 800 µmol N flask^{-1}). Panel C. Growth
798 from complete denitrification (NO_3^- to N_2; initial amount of NO_3^- was 200 µmol flask^{-1}). Panel D. Yield per
799 mol e^- obtained from growth using the different electron acceptors. The differences in yield were
800 statistically different ($p<0.01$). O_2 was depleted in the O_2 treatment after 55 h, while N_2O and NO_3^- were
801 not depleted during the incubations. Bars indicate standard deviation, n=3. Note: The initial value for DW,
802 estimated by cumulated electron flow, was set equal to that based on measured OD.

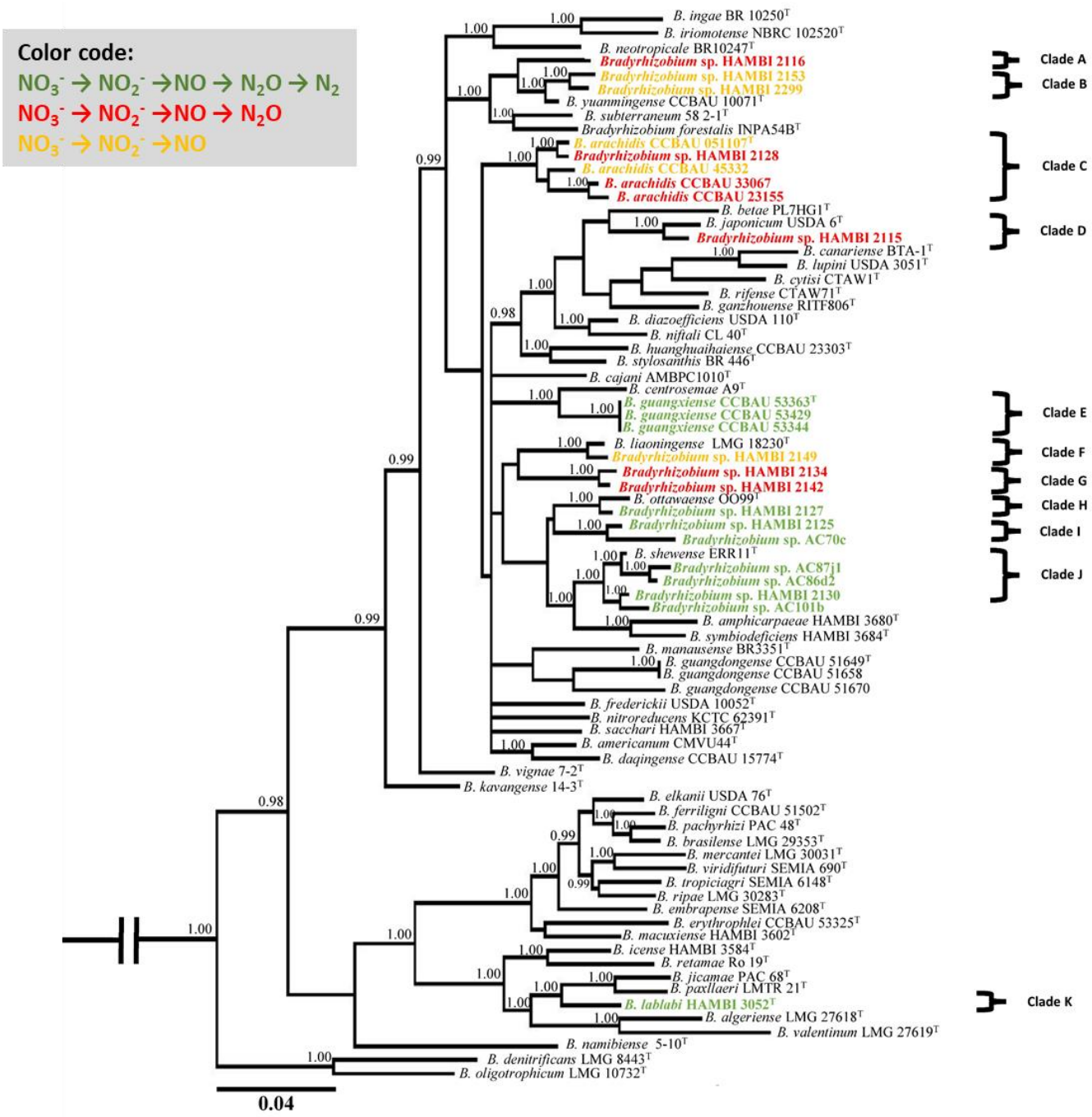

Fig. 1. Phylogenetic tree of four concatenated housekeeping genes (*atpD- glnII- recA- rpoB*) from 78 *Bradyrhizobium* strains constructed based on a Bayesian inference analysis. Only the posterior probabilities ≥0.95 are shown in the tree. The genus name *Bradyrhizobium* is abbreviated as *B.*, and a "T" at the end of each strain code shows the type strains. In cases where two or more isolates showed high whole genome sequence similarity (>99 %) based on pairwise comparison of Average Nucleotide Identity (ANI) (see Table S1), only one representative is shown in this tree. Colors indicate denitrification end-products. A sequence analysis of the genes in the respective denitrification gene operons showed good correspondence between genetic set-up and denitrification end products (Table S2). The only exception was HAMBI 2299, which had a complete *nor* operon but did not reduce NO. Another non-NO reducing strain, HAMBI 2153, lacked two genes in the *nor* operon.

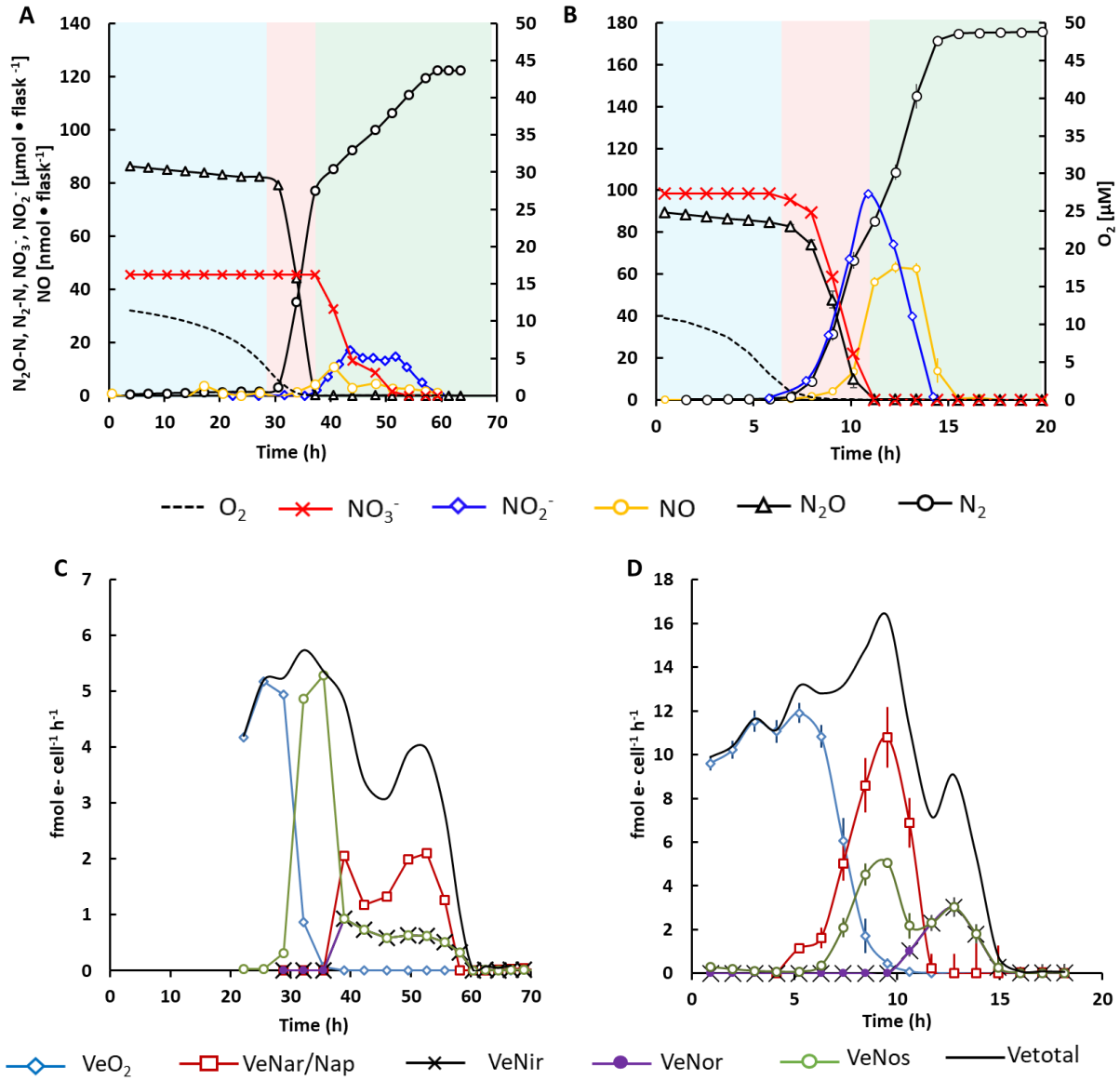

Fig. 2. Competition for electrons between N_2O- and NO_3^- reductase; comparison of Nap- and Nar-carrying organisms. Gas kinetics and corresponding electron flow to oxidases (aerobic respiration) and to the different N-reductases (denitrification) in batch cultures of *Bradyrhizobium* strain HAMBI 2125 and *Paracoccus denitrificans*. Both organisms perform complete denitrification but *Bradyrhizobium* carries only the periplasmic NapA for dissimilatory NO_3^- reduction while *P. denitrificans* carries both NapA and the membrane-bond NarG. The top panels (A, B) show the measured amounts of NO_2^-, NO, N_2O and N_2 per flask, and the concentration of O_2 in the liquid. Note that the small but significant decrease in N_2O during the aerobic phase was caused by sampling losses, not by N_2O reduction or other reactions, as explained in Fig. S6. Background colors indicate the dominating respiratory activity. Blue: O_2 respiration; Pink: N_2O respiration; Green: Complete denitrification (NO_3^- to N_2). The bottom panels (C, D) show the calculated cell specific rates of electron flow (fmol $cell^{-1}$ h^{-1}) to the terminal oxidases (V_{eO2}) and to the four reductases ($V_{eNar/Nap}$, V_{eNir}, V_{eNor} and V_{eNos}). V_{eNir} and V_{eNor} were practically identical throughout (NO remained very low), thus indistinguishable in the panels. Strain HAMBI 2125 was incubated in 4 replicate flasks with YMB supplemented with 1 mM KNO_3, of which only one is shown here (gas- and NO_2^- kinetics of replicate flasks are shown in Fig. S3). *P. denitrificans* was incubated in 50 ml Sistrom's medium with 2 mM KNO_3 (n=7, bars show standard errors). At the start of the incubation, all flasks contained ~1% O_2 in the headspace (~10 µM in liquid) and ~ 1.2 ml N_2O

(~90 µmol N_2O-N). $V_{eNar/Nap}$ and V_{eNir} represent rates of electron transport to NO_3^- and NO_2^-, respectively (via NapA and NirK for *Bradyrhziobium* and via NarG+Nap and NirS for *P. denitrificans*).

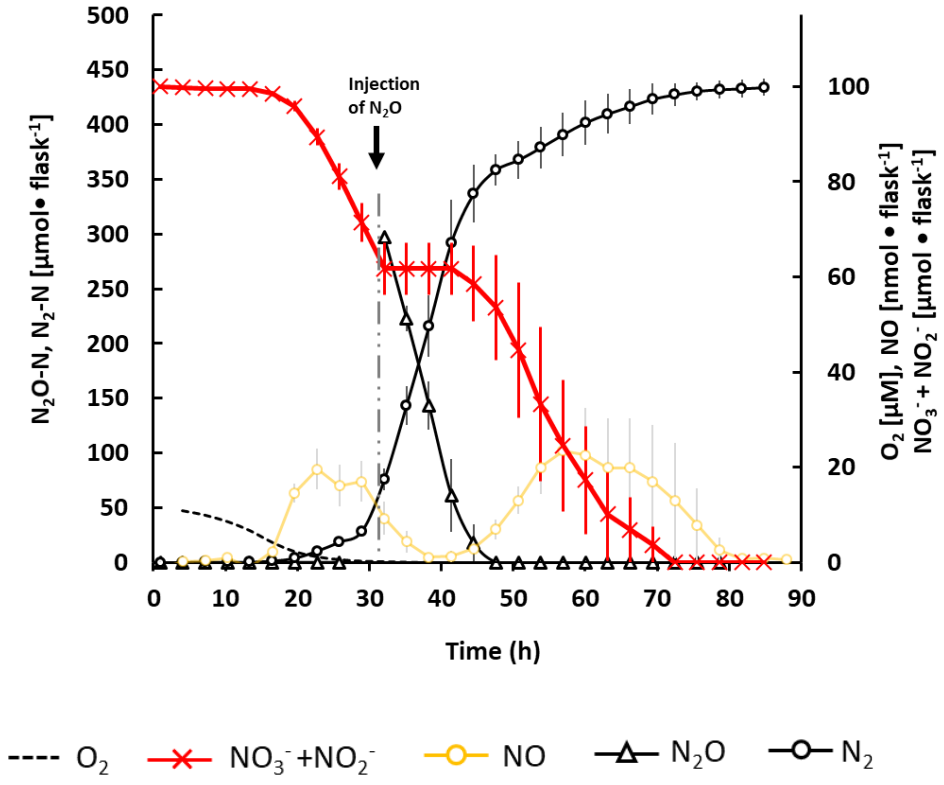

Fig. 3. Effect of injecting N_2O to an actively denitrifying culture. Gas kinetics for *Bradyrhizobium* strain HAMBI 2125 during and after transition from aerobic respiration to N-oxide respiration. Triplicate cultures were incubated in YMB medium supplemented with 2 mM KNO_3 and with 0.7 ml O_2 in the headspace (around 10 µM O_2 in the medium). Approximately 4 ml N_2O (~300 µmol N_2O-N) were injected at 32 hpi, indicated by the arrow, into actively denitrifying cultures respiring NO_3^-. Bars show standard errors (n=3).

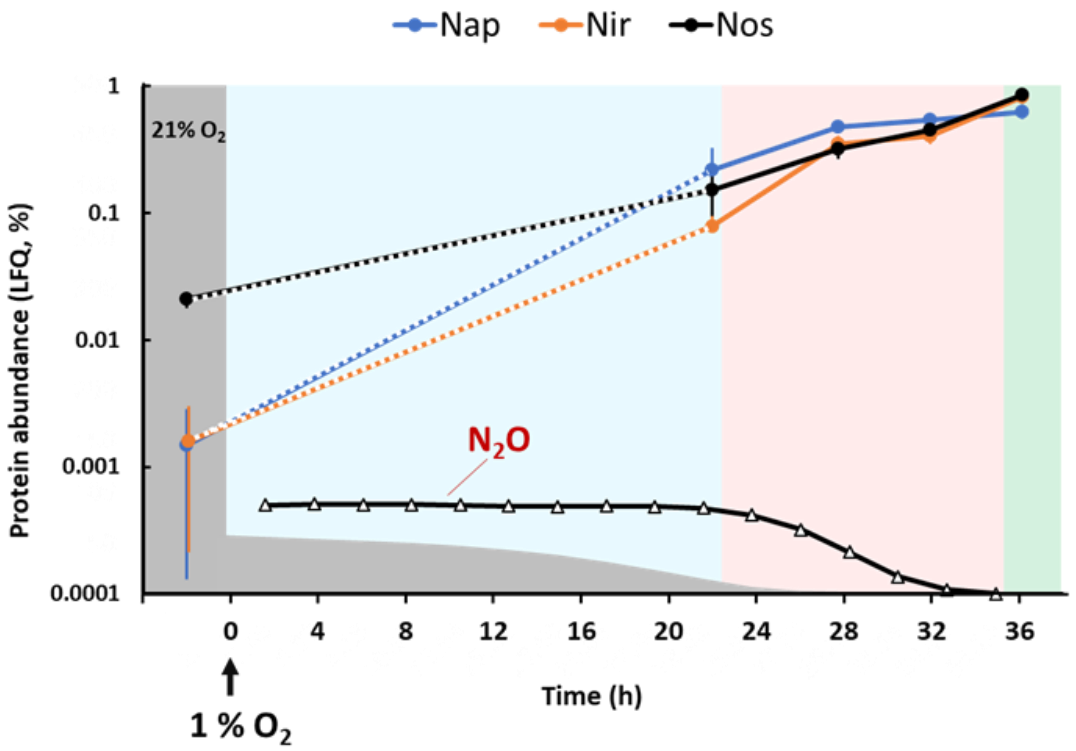

Fig. 4. Abundance of denitrification reductases during and after transition from aerobic to anaerobic respiration. The abundances of Nap, NirK and Nos were determined by proteomics and calculated as percentages of the sum of all LFQ (label-free quantitation of proteins) abundances for each time point. The first samples were taken from triplicate flasks of *Bradyrhizobium* strain HAMBI 2125 growing under fully oxic conditions (21% O_2). Subsamples from these precultures were inoculated into flasks with 1% O_2, and samples for proteomics were taken when the cultures approached O_2 depletion ([O_2] = 5.8±0.2 µM) and during the anaerobic respiration. Concentrations of O_2 (grey shading) and N_2O (-Δ-) are schematically indicated here to illustrate the time of their depletion; for actual values of [O_2] [N_2O], [N_2] and [NO_2^-], see Fig. S8. Background colors indicate the dominating respiratory activity. Blue: O_2 respiration; Pink: N_2O respiration; Green: Complete denitrification (NO_3^- to N_2). Bars show standard deviation (n=3).

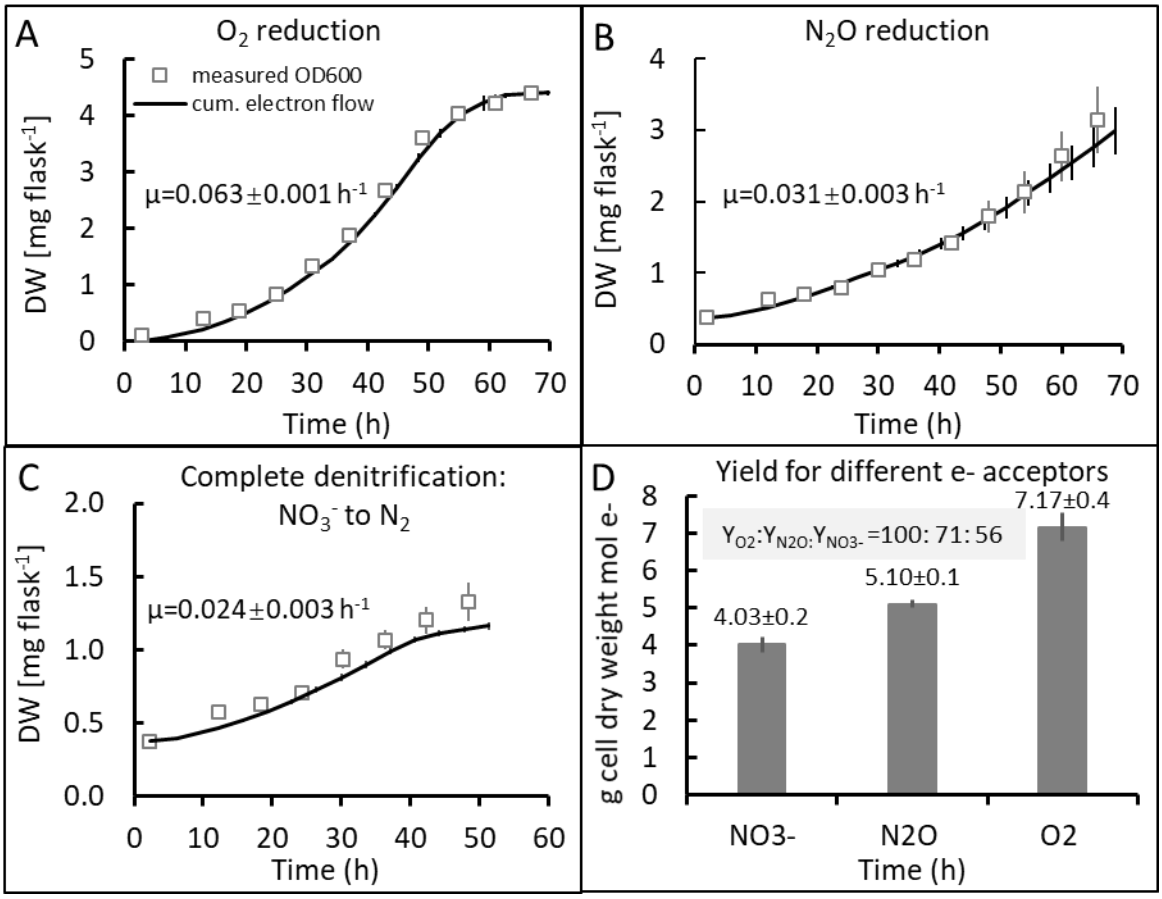

Fig. 5. Growth and yield of *Bradyrhizobium* strain HAMBI 2125 when incubated in YMB at 28 °C and provided with O_2, N_2O or NO_3^- as electron acceptor. All relevant gases were measured frequently using a robotized system. Panels A-C show estimated g dry weight (DW) flask^{-1} throughout the incubations either calculated from measured OD_{600} (□) using the factor 0.374 mg dry weight ml^{-1} OD_{600}^{-1} (Fig. S7) or calculated from the measured cumulated electron flow (solid line) using measured yields per mol e^- in panel D. The specific growth rates (μ) were determined by regression of ln(OD_{600}) against time during the period of exponential growth. Panel A. Growth using O_2 as sole electron acceptor (initial amount 180 μmol flask^{-1}). Panel B. Growth using N_2O as sole electron acceptor (initial amount 800 μmol N flask^{-1}). Panel C. Growth from complete denitrification (NO_3^- to N_2; initial amount of NO_3^- was 200 μmol flask^{-1}). Panel D. Yield per mol e^- obtained from growth using the different electron acceptors. The differences in yield were statistically different ($p<0.01$). O_2 was depleted in the O_2 treatment after 55 h, while N_2O and NO_3^- were not depleted during the incubations. Bars indicate standard deviation, n=3. Note: The initial value for DW, estimated by cumulated electron flow, was set equal to that based on measured OD.

Table 1. Strains used in the current study. All listed strains were included in the MLSA-based phylogenetic analysis (Fig. 1). The strains above the dashed line were also examined in the present study with regard to their denitrification phenotypes. Strains AC 70c, AC 86d2, AC 86j1 and AC 101b were not examined for denitrification since this was reported elsewhere (Mania *et al*., 2020).

Strain*	Host plant	Geographic origin	Reference
HAMBI 2115	*Arachis hypogaea* L.	Zimbabwe	(Zhang *et al*., 1999)
HAMBI 2116	*A. hypogaea* L.	Zimbabwe	(Zhang *et al*., 1999)
HAMBI 2125	*A. hypogaea* L.	Sichuan, China	(Zhang *et al*., 1999)
HAMBI 2127	*A. hypogaea* L.	Sichuan, China	(Zhang *et al*., 1999)
HAMBI 2128	*Macrotyloma africanum*	Zimbabwe	(Van Rossum *et al*., 1993)
HAMBI 2130	*Vigna unguiculata*	Zimbabwe	(Van Rossum *et al*., 1994)
HAMBI 2134	*A. hypogaea* L.	Sichuan, China	(Zhang *et al*., 1999)
HAMBI 2142	*A. hypogaea* L.	Sichuan, China	(Zhang *et al*., 1999)
HAMBI 2149	*A. hypogaea* L.	Sichuan, China	(Zhang *et al*., 1999)
HAMBI 2153	*A. hypogaea* L.	Israel	(Zhang *et al*., 1999)
HAMBI 2299	*A. hypogaea* L.	Hawaii, USA	HAMBI**
HAMBI 3052^{T}	*Lablab purpureus*	Anhui, China	(Chang *et al*., 2011)
CCBAU 051107^{T}	*A. hypogaea* L.	Hebei, China	(Wang *et al*., 2013)
CCBAU 23155	*A. hypogaea* L.	Anhui, China	(Wang *et al*., 2013)
CCBAU 33067	*A. hypogaea* L.	Jiangxi, China	(Wang *et al*., 2013)
CCBAU 45332	*A. hypogaea* L.	Henan, China	(Wang *et al*., 2013)
CCBAU 53344	*A. hypogaea* L.	Guangxi, China	(Li *et al*., 2015)
CCBAU 53363^{T}	*A. hypogaea* L.	Guangxi, China	(Li *et al*., 2015)
CCBAU 53429	*A. hypogaea* L.	Guangxi, China	(Li *et al*., 2015)
AC70c	*Phaseolus vulgaris*	Akaki, Ethiopia	(Degefu et al., 2017)
AC86d2	*Cajanus cajan*	Awassa, Ethiopia	(Degefu et al., 2017)
AC87j	*Millettia ferruginea*	Awassa, Ethiopia	(Degefu et al., 2017)
AC101b	*Acacia saligna*	Leku, Ethiopia	(Degefu et al., 2017)

HAMBI: The culture collection at the Department of Microbiology, University of Helsinki.
CCBAU: Culture Collection of China Agricultural University, Beijing, China.
AC: The strains are kept in a local collection at Norwegian University of Life Sciences and available upon request (Å. Frostegård).
*) For information on donator and specimen history of HAMBI strains please consult https://kotka.luomus.fi/culture/bac
**) https://kotka.luomus.fi/view?uri=http://tun.fi/RAH.1747&type=document&page=1&spot=1